

## CHAPTER 3

### COVALENT GRAFTING NITROGEN-BIOMOLECULES ONTO PLASMA-MODIFIED POLYSTYRENE CULTURE DISH USED FOR SERUM-FREE CONDITION

#### 3.1 Introduction

The development of cell therapy using mesenchymal stem cells (MSCs) can be achieved by transplantation of cells in plenty numbers and quality, to treat many human diseases [1]. Nowadays, *In vitro* mammalian cell culture, mammal-derived factors including fetal bovine serum (FBS) are often used as a growth supplement and growth factors in the media which cause the concern about the risk of infection [2, 3]. Therefore, serum- and mammal-free culture is strongly required. We focused on sericin hydrolysates, a protein extracted from the glue of cocoons, with the alternative strategy of being used as supplemented in the culture media. Silk proteins were added to culture media used as serum free media for cell culture. Additionally, it was coated onto Petri dishes which resulted in enhanced attachment of cultured human skin fibroblasts [4]. In comparison with bovine serum albumin (BSA), sericin had an equivalent effect on the proliferation of the hybridomas with BSA and the activity of sericin was not affected by autoclaving. Commonly, sericin protein absorbed onto various substrates spontaneously, however, sericin itself is water soluble. In the case of cell culture application, their immediately removal from the surface when exposed to the culture media and could not support the cell growth for a prolonged time.

Polystyrene (PS) has been used since 1965 [5] as a popular culture vessels for microbes due to its excellent durability, good optical and non-toxicity. The Tissue culture polystyrene (TCPS), as a standard *in vitro* cell culture substrates, is unsuitable for serum free cell culture medium since it normally occur in a poor and insufficiently reproducible manner [6]. Therefore, surface modifications are required to optimize cell adhesion and accelerate the cell proliferation. Amorphous carbon (a-C) is now being attractive in biological applications because it can be prepared relatively inexpensively for a wide variety of low-cost precursors. It is typically biocompatible and quite chemically stable under nonoxidizing conditions. Moreover, it has low density, high thermal conductivity, good electrical conductivity, mechanical stability and is non cytotoxic. Of prominent features of the carbon film including a high specific-area, porous carbon is a more binding active molecule and more resistant to structural change by hydrolytic effects in aqueous environments.

It is well known that attachment in the first stage is controlled by the interaction between cell and surface materials, while the longer term adhesion and proliferation are associated with the presence of specific biological molecules and/or proteins [7-9]. Mechanism of immobilization biomolecules by covalent bond offers several advantages by providing the most stable bond between the biomolecule and the functionalized polymer surface. The surface-immobilized biomolecules with chemical bond could lead to permanent or long-term retention. For covalent binding to an inert solid polymer surface, the surface must first be modified to provide reactive groups (e.g.  $-OH$ ,  $-NH_2$ ,  $-COOH$ ,  $-SH$  or  $-CH=CH_2$ ) for the subsequent immobilization step [7, 10, 11]. In the case of cell culture applications, a covalent linkage ensure that the bioactive compound will not be suddenly removed from surface when exposed to the culture media or migrate to the culture media for a period of a long time.

This review therefore selectively focuses on a new method of immobilization bioactive compounds onto polymer surface via deposited-carbon films (Figure 3.1). Many types of carbon-based films were grown by physical vapor deposition in a DC magnetron plasma sputtering system and a RF plasma-enhanced chemical vapor deposition (PECVD) system. The deposited-carbon films were used as an intermediate layer for sericin grafting onto PS surface. The objective of this study is to investigate and discuss the interaction between PS surface - Intermediate layer - Silk coating and attempt to control and slow down the release rate of coated-silk molecules by chemical bond between protein molecules and PS surface.

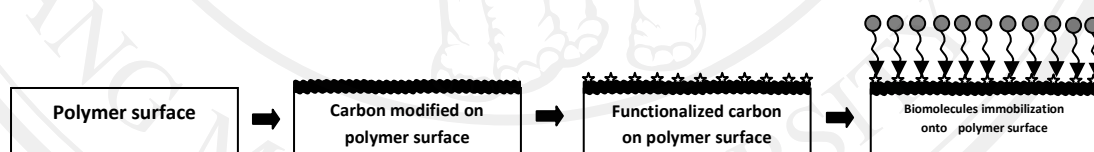


Figure 3.1 Concept of biomolecules immobilization onto modified surface.

### 3.2 Experimental Setup and Methods; Amorphous Carbon Deposition Coatings by Magnetron Sputtering System

In this study, we investigate the effects of different types of plasma treatment: nitrogen- and silicon dioxide-plasma on the biocompatibility of a-C films, based on the covalent grafting of sericin molecules and the cellular attachment and proliferation of human bone marrow mesenchymal stem cells (hBM-MSCs).

### 3.2.1 Physical Vapor Deposition (PVD) Sputtering System

Commercialize TCPS dishes (Nunclon®, Denmark; Cat#153066), 35 mm in diameter, were used as the material model in this study. The bottom part of each dish was used in this experiment as modified PS dish with amorphous carbon-based intermediate layer.

To manipulate the amorphous carbon-based films, we used a DC magnetron sputtering system (Figure. 3.2) (Center for Advanced Plasma Surface Technology; CAPST, Sungkyunkwan University, Korea) attached to a high vacuum chamber (base pressure  $2 \times 10^{-5}$  Torr) using a 4-inches diameter high purity carbon target cathode and argon (purity 99.999%) gas as a working gas. The a-C films deposited onto the PS bottom part was used for the SiO<sub>x</sub> deposition as a-C:SiO<sub>x</sub> films and was used for the nitrogen plasma treatment as a-C:N<sub>2</sub> films by using a RF plasma-enhanced chemical vapor deposition (PECVD) system (as described by Su B. Jin, 2011 [12]). Table 3.1 lists the sputtering deposition parameters.

Table 3.1 Sputtering parameters.

Parameters	Conditions
Base pressure	About $2.0 \times 10^{-5}$ Torr
Sputtering pressure; 1) a-C <sub>1</sub>	$1.2 \times 10^{-1}$ Torr
2) a-C <sub>2</sub>	$1.3 \times 10^{-1}$ Torr
DC power	0.5 and 0.8 kW
Sputter time	10, 15 and 20 min

### 3.2.2 Plasma-enhanced Chemical Vapor Deposition (PECVD) System

To functionalize of carbon film surfaces by using a RF PECVD system (Figure 3.3) with SiO<sub>x</sub> plasma using octamethylcyclotetrasiloxane (OMCTS) as a precursor and oxygen as a carrier gas after that we used oxygen plasma treated onto SiO<sub>x</sub> films to improve the hydrophilic and used as the a-C:SiO<sub>x</sub> films. In case of a-C:N<sub>2</sub> films, we used nitrogen plasma treated onto a-C films. Table 3.2 lists the deposition parameters.

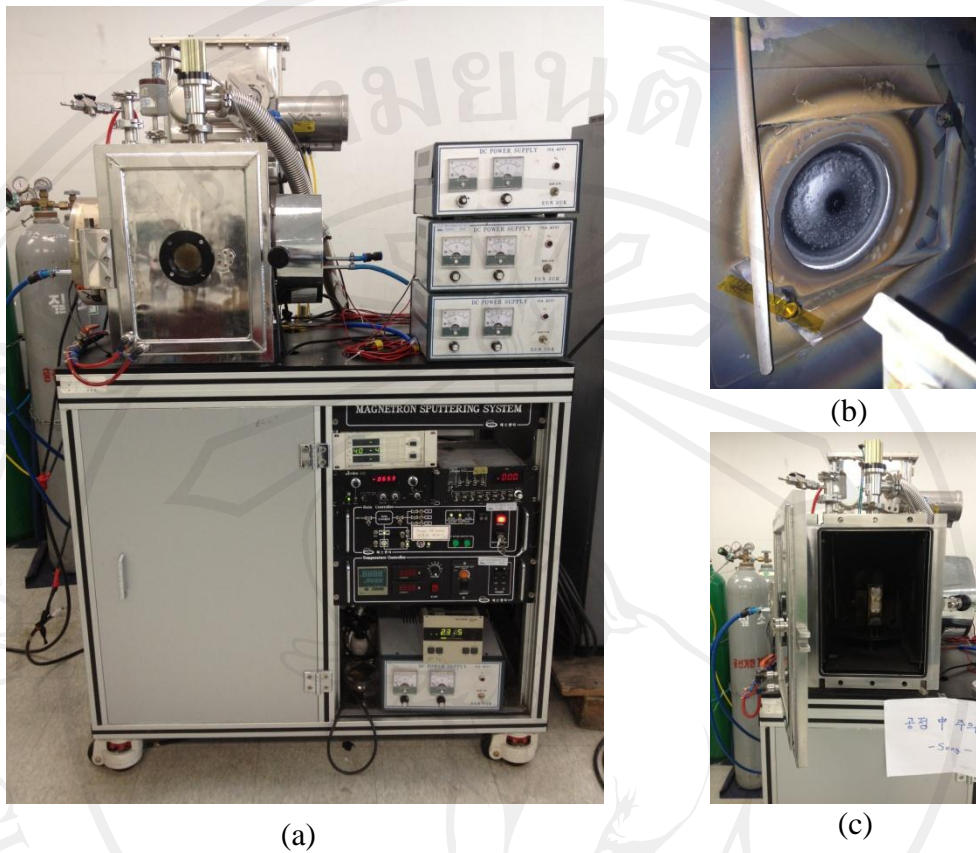


Figure 3.2 DC magnetron sputtering system (a), a carbon target (b) and PS dishes placed on sample holder (c).

Table 3.2 Deposition parameters.

Parameters	Conditions
Base pressure	About $3.0 \times 10^{-2}$ Torr
Deposition pressure;	$1.0 \times 10^{-1}$ Torr
1) SiO <sub>x</sub> deposition	
Top electrode (RF, 13.56 MHz)	140 W
Bottom electrode (RF, 13.56 MHz)	100 W
2) O <sub>2</sub> plasma treatment	100 W
3) N <sub>2</sub> plasma treatment	80 W
Deposition time	1 min
Temperature	Room temperature
Distance between top electrode and substrate	70 mm

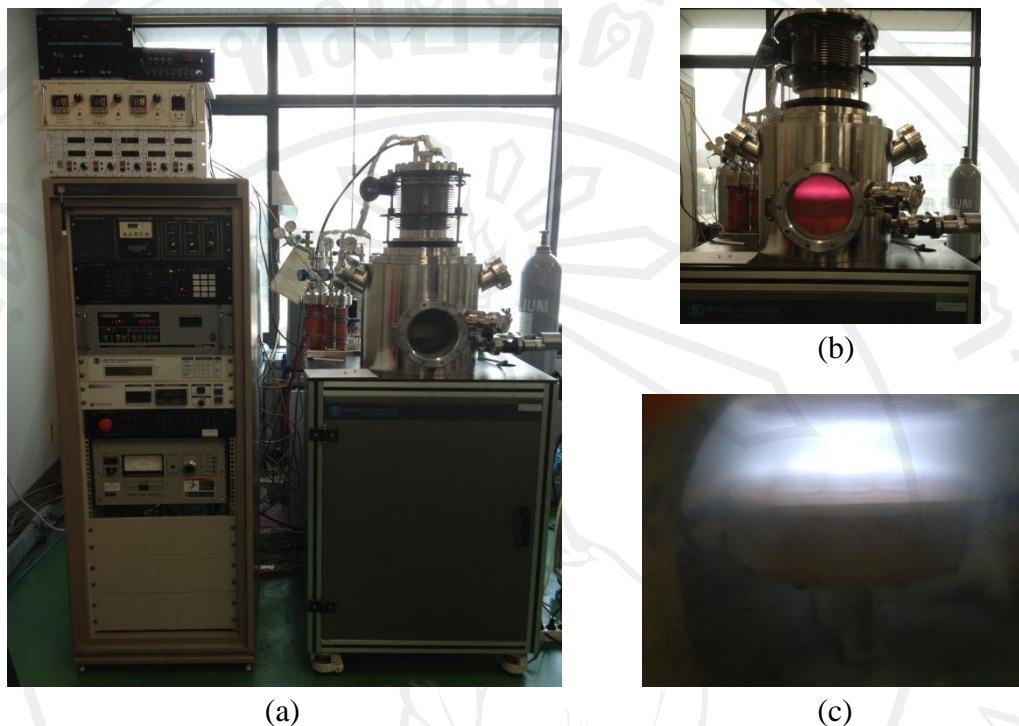


Figure 3.3 A RF PECVD system (a), plasma discharge (b) and PS dishes placed on bottom electrode (c).

### 3.3 Protein Biomolecule Immobilization onto Plasma-modified PS Dish

The active sites formed in a polymer surface during plasma functionalization processes. In our recent study, polystyrene (PS) were modified by carbon sputtering. The plasma sputtering is able to exert four major effects: (i) surface cleaning, (ii) surface ablation or etching, (iii) surface cross-linking, and (iv) modification of the surface chemical structure. Plasma treatment leads to cleavage of C-C and C-H bonds. This results in splitting of macromolecules, and free radicals and conjugated double bonds are generated on the polymer chain. The degradation products of macromolecules also react with the oxygen present in the ambient atmosphere in the chamber and create oxidized structures, e.g. carbonyl, carboxyl and ester groups, which increase the polarity and wettability of the polymer surface [13, 14]. Oxidized degradation products are produced on the polymer surface, contributing to increased hydrophilicity (wettability) of the plasma treated polymers. In PS with a lower crystalline fraction, the tiny, sharp formations appearing after plasma treatment may represent low molecular, oxidized structures (LMWOS) [15]. The surface of the plasma-activated polymer with amorphous carbon films was grafted with sericin molecules (as described in 3.4.2).

### 3.4 Evaluation

Modified surfaces were characterized by fourier transform infrared (FTIR) spectroscopy, x-ray photoelectron spectroscopy (XPS), atomic force microscopy (AFM), scanning electron microscope (SEM) and contact angle measurement. We also investigated the short-term effect, over 7 days, on the UV-vis absorbance of the released-sericin solution. For the cell assay, we investigated on cellular behavior including attachment efficiency and proliferation rate of human bone marrow-derived mesenchymal stem cells (hBM-MSCs) in serum and serum-free condition on carbon-based PS surfaces compared with commercial PS culture dishes namely tissue culture polystyrene (TCPS).

#### 3.4.1 Physico-chemical Properties Study

Contact angle was obtained using the sessile drop technique with DI water droplet of 20  $\mu\text{l}$ . A micropipette was used to drop the water on the surface of PS-membrane samples. The image of the water droplet was then captured and exported to an image analyzing software to determine the contact angle. Water contact angle measurement demonstrates the relationship between the properties and chemistry of a surface by wettability. The contact angle (in degrees) is the angle at which a liquid interface meets a solid surface. The greater the angle, the higher is the surface hydrophobicity.

Atomic force microscope (SHIMADZU SPM-9500 J2, Japan) was used for morphological characterization of carbon base modified-PS surfaces. The image measurement was performed in tapping mode. The scan rate used was as 1 Hz in air.

An ATR-unit of a Nicolet OMNI-Sampler Smart Accessory FTIR spectrophotometer was used to investigate chemical bond on the sample surfaces. The spectra were collected by averaging 64 scans at a resolution of 4  $\text{cm}^{-1}$  from 400-4000  $\text{cm}^{-1}$ .

X-ray photoelectron spectroscopy (XPS) was carried out to determine the quantitative and qualitative elemental surface composition, using an Ultra DLD spectrometer (Kratos Analytical Ltd, UK) with a monochromatized Al- $\text{K}_{\alpha}$  x-ray source ( $h\nu = 1486.6 \text{ eV}$ ). The anode voltage and current were 15 kV and 10 mA. Survey spectra were collected using a pass energy of 160 eV with 1 eV/step, while region scans were collected with a pass energy of 40 eV, at a rate of 0.1 eV/step. The pressure in the analysis chamber was maintained at  $7 \times 10^{-7} \text{ Pa}$ . Binding energy was referenced to the C1s neutral carbon peak at 284.6 eV.

### 3.4.2 The Sericin Release Rate Detection Using Ultraviolet (UV) Absorption

#### 1) Immobilization Method

Sericin powder (Thailand Institute of Nuclear Technology; TINT as shown in Figure 3.4a) was dissolved in DI water as 5.0% *w/v* solution and stirred at 60-70 °C for 30 min. 100  $\mu$ l of sericin solution was dropped and spread into each PS dish, let dry in air for 24 h (Figure 3.4 b). After that, 7 ml of phosphate buffer saline (PBS) solution was poured into each sericin coated-PS dish and allowed the immersed time for 1, 3, 5 and 7 days (*n*=4 for each), as shown in Figure 3.5, 3.6 and 3.7.

#### 2) Measurement The UV Absorbance of The Released-sericin Solution

UV spectra of the released-sericin solution were taken on a UV-VIS-NIR spectrophotometer (UV-3600, Shimadzu, Tokyo, Japan). Kept 3 ml of released-sericin solution transferred to the quartz cuvette with a 1-mm pathlength and scanned with the scanning range was recorded between 190 -450 nm.

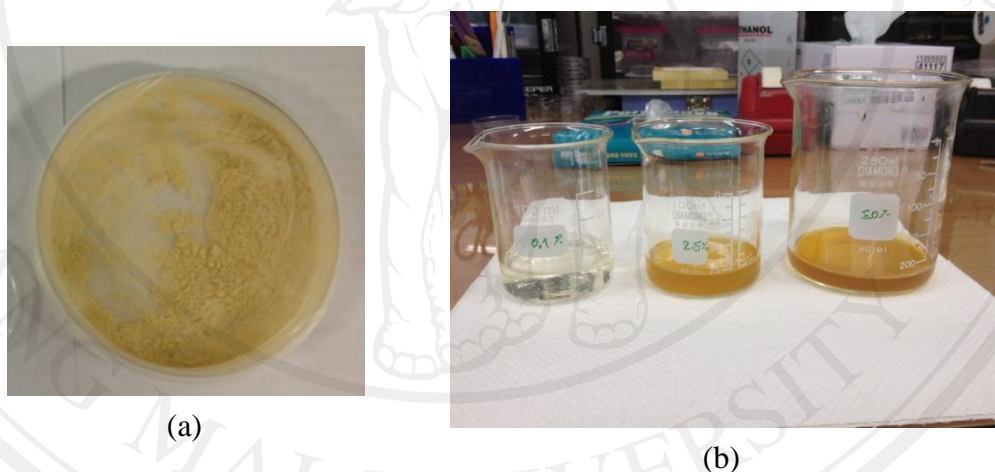


Figure 3.4 Silk sericin powder (a) and silk sericin solution (b).

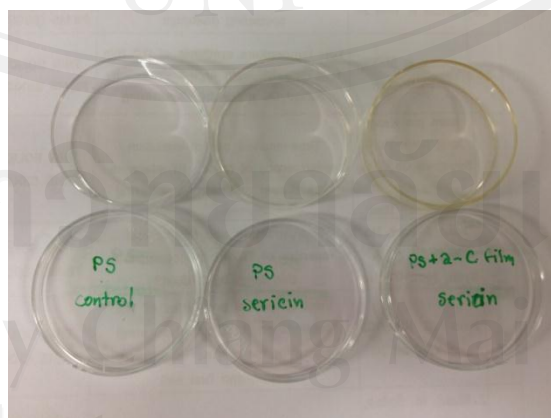


Figure 3.5 PS Petri dishes control, PS+sericin coating and PS-modified+sericin, respectively.



Figure 3.6 Various PS Petri dish with PBS immersed for the release rate detection.

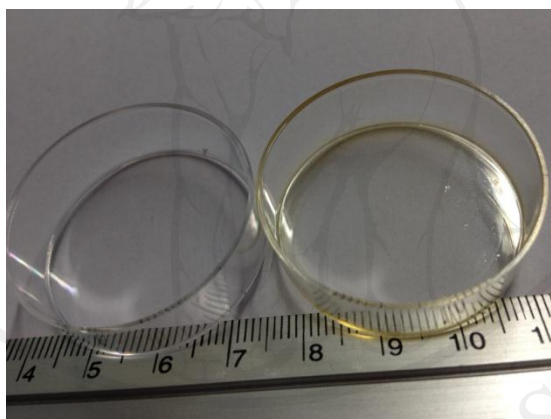


Figure 3.7 PS Petri dish control and PS modified surface.

### 3.4.3 Cell Behavior Study

#### 1) Cell Culture and Seeding

The human bone marrow-derived mesenchymal stem cells (hBM-MSCs) were purchased from Lonza group Ltd., Switzerland. The cells were cultured on 75  $cm^2$  PS cultured flasks (SPL®, Korea; Cat#70025) in DMEM (Dulbecco's modified Eagle's medium) (Gibco, USA) containing 20% ( $v/v$ ) FBS (fetal bovine serum) (Gibco, USA) and 1% penicillin/streptomycin (Pen Strep, Gibco, California, USA) for serum condition and not use FBS for serum-free condition. Cultures were maintained at 37°C, 5% CO<sub>2</sub> and 95% relative humidity. The culture medium was refreshed every 2 days before achieving 80% cell-population confluence. On detaching from



the culture flasks, they were exposed to 0.05% (*v/v*) trypsin-EDTA (Gibco, USA) for 3 min. The cells were collected and washed with phosphate buffer saline (PBS) then centrifuged and re-suspended in the medium prior to cell seeding.

### 2) Cell Attachment Efficiency and Proliferation Assay

Attachment efficiency and proliferation assay of hBM-MSCs were quantitatively evaluated by using the WST-1 reagent (Roche, USA). Cells were plated at a density of  $1 \times 10^4$  cells per dish (PS control and PS modified surface as shown in Figure 3.7). According to the manufacture's instruction, 150  $\mu$ l of WST-1 solution was added to each dish and incubated at 37°C for 4 h. The colorimetric optical density (OD) of liquid in each dish was obtained by spectrophotometry at 450 nm using Epoch (Biotek, USA). The proliferation assay was analyzed using the OD450 value from each PS dish sample at day 1 and day 7 in comparison to the control at day 1, which was presented as percentage of attached and proliferated cells. A higher percentage of cell attachment and proliferation corresponds to a higher number of viable cells.

### 3) Cell Morphology

A scanning electron microscope (SEM) (S-800, Hitachi, Ltd., Japan) was also used to observe the fine details of the attachment mechanism of cells on the surfaces.

## 3.5 Results and Discussion

### 3.5.1 Surface Characterization

The surface hydrophilicity of modified PS dish was improved by amorphous carbon (a-C) deposition and was significantly improved by using  $\text{SiO}_x$  deposition and nitrogen plasma treatment. A different a-C films; vary of DC power and Ar pressure, had lower contact angle of less than 50° (compared with 82° for the PS-control) and a-C: $\text{N}_2$  films had lower contact angle of 25°. A-C: $\text{SiO}_x$  films had a great lower contact angle of less than 10°, indicating good spreading of water on the material surface and low hydrophobicity of the material surface (Table 3.3). The deposited of  $\text{SiO}_x + \text{O}_2$  treatment and nitrogen treatment resulted in more polar groups (oxidized structures e.g. carbonyl, carboxyl and ester groups and *Si-O*, *NH*<sub>2</sub>) being grafted onto the PS surface during the plasma process. This geometrical appearance is unsuitable for binding to cells, since specific sites on these molecules are less accessible to cell adhesion receptors, e.g. integrin. The polar component of surface energy consists of all other interactions due to non-London forces. Polar molecules interact through dipole-dipole intermolecular forces and hydrogen bonds. On hydrophilic surfaces, cells adhered in higher numbers to more hydrophilic materials and were spread over a large area. At the same time, ECM proteins were adsorbed in a more flexible form,

which allows them to be rearranged by the cells and thus provides access for cell adhesion receptors to the adhesion motifs on these molecules.

In these experiments, the a-C<sub>1</sub> and a-C<sub>2</sub> films thickness of approximately 35 nm and 25 nm, respectively (sputter time: 10 min) were measured by surface profiler Alpha-step IQ (Table 3.3). The a-C<sub>2</sub>:N<sub>2</sub> film thickness was about 110 nm (sputter time: 10 min and N<sub>2</sub> treatment time: 1 min). In the case of a-C:SiO<sub>x</sub> films, the thickness were 157 nm for a-C<sub>1</sub>:SiO<sub>x</sub> film, 95 nm for a-C<sub>2</sub>:SiO<sub>x</sub> film (sputter time: 10 min and SiO<sub>x</sub> treatment time: 1 min and O<sub>2</sub> treatment 1 min). It was also shown that SiO<sub>x</sub> deposition and nitrogen plasma treatment can increase the film thickness and the hydrophilic of carbon films.

Table 3.3 Films thickness and contact angle.

Plasma modified-PS surfaces	Film thickness (nm)	Contact angle (°) ±SD
PS control	-	82 ± 1.4
PS + a-C <sub>1</sub> film	35	43 ± 2.5
PS + a-C <sub>2</sub> film	25	46 ± 2.0
PS + a-C <sub>1</sub> :SiO <sub>x</sub> film	157	14 ± 2.0
PS + a-C <sub>2</sub> :SiO <sub>x</sub> film	94	19 ± 2.0
PS + a-C <sub>2</sub> :N <sub>2</sub> film	110	25 ± 1.5

SEM images showed the morphology of the various a-C based-film surfaces in Figure 3.8. It is shown that the a-C films fabricated by the lower DC power at 0.5 kW (a) had the quite more dense films than the higher DC power 0.8 kW (b). The warped deformation observed at the longer sputter time due to the heat of carbon atoms bombarded on surface as shown in figure (c) and (d).

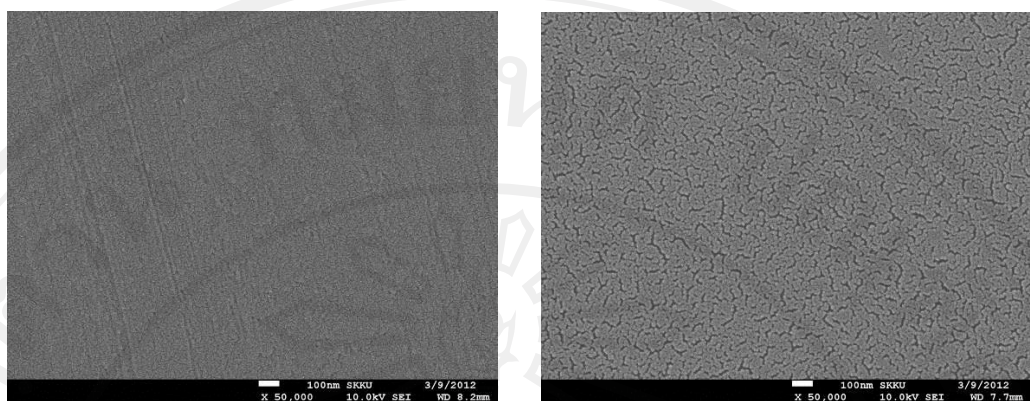
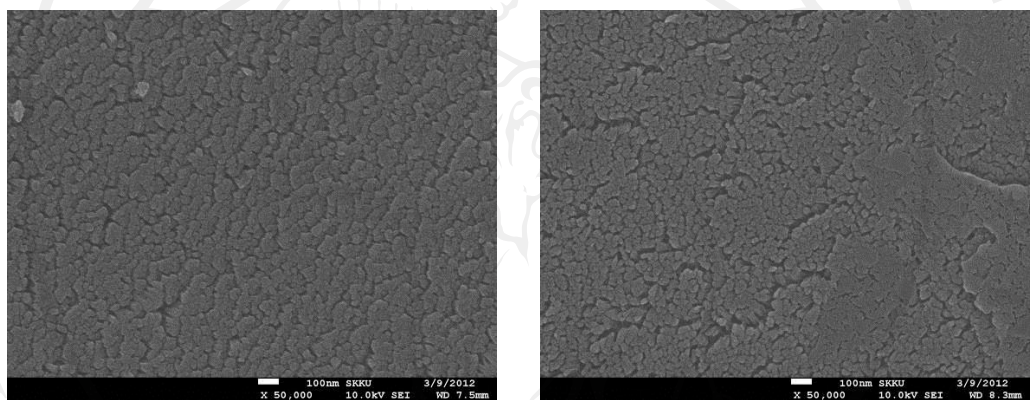
a) a-C film; 0.5 kW, Ar  $1.3 \times 10^{-1} T$ , 10 minb) a-C film; 0.8 kW, Ar  $1.3 \times 10^{-1} T$ , 10 minc) a-C film; 0.8 kW, Ar  $1.3 \times 10^{-1} T$ , 20 mind) a-C film; 0.8 kW, Ar  $1.3 \times 10^{-1} T$ , 30 min

Figure 3.8 SEM images of a-C surfaces with variable DC power and sputter time.

We also studied the variable of Ar pressure effect on the morphology of a-C films. It is shown that the a-C with lower Ar pressure at  $1.2 \times 10^{-1} Torr$  was quite dense and smooth films (Figure 3.9a), whereas, the a-C with higher Ar pressure at  $1.3 \times 10^{-1} Torr$  was a homogeneous distribution of nanoscale holes surface (Figure 3.9b) and also shown in the case of a-C:N<sub>2</sub> films too (figure 3.9c). The nanoscale hole distribution of a-C surface increased surface area and great impact on the behavior of protein adsorption on carbon surface. However, the a-C:SiO<sub>x</sub>-based films (Figure 3.9d) were dense and smooth films after SiO<sub>x</sub> deposition onto a-C films. It can be imply that the Si-O functional groups affect to the hydrophilic property of PS surface more than carbon surface roughness, based on the contact angle data (Table 3.3). Nevertheless, the pore size and surface area has great impact on the behavior of adsorption on carbon materials, higher surface area highly adsorb proteins and so on. [16].

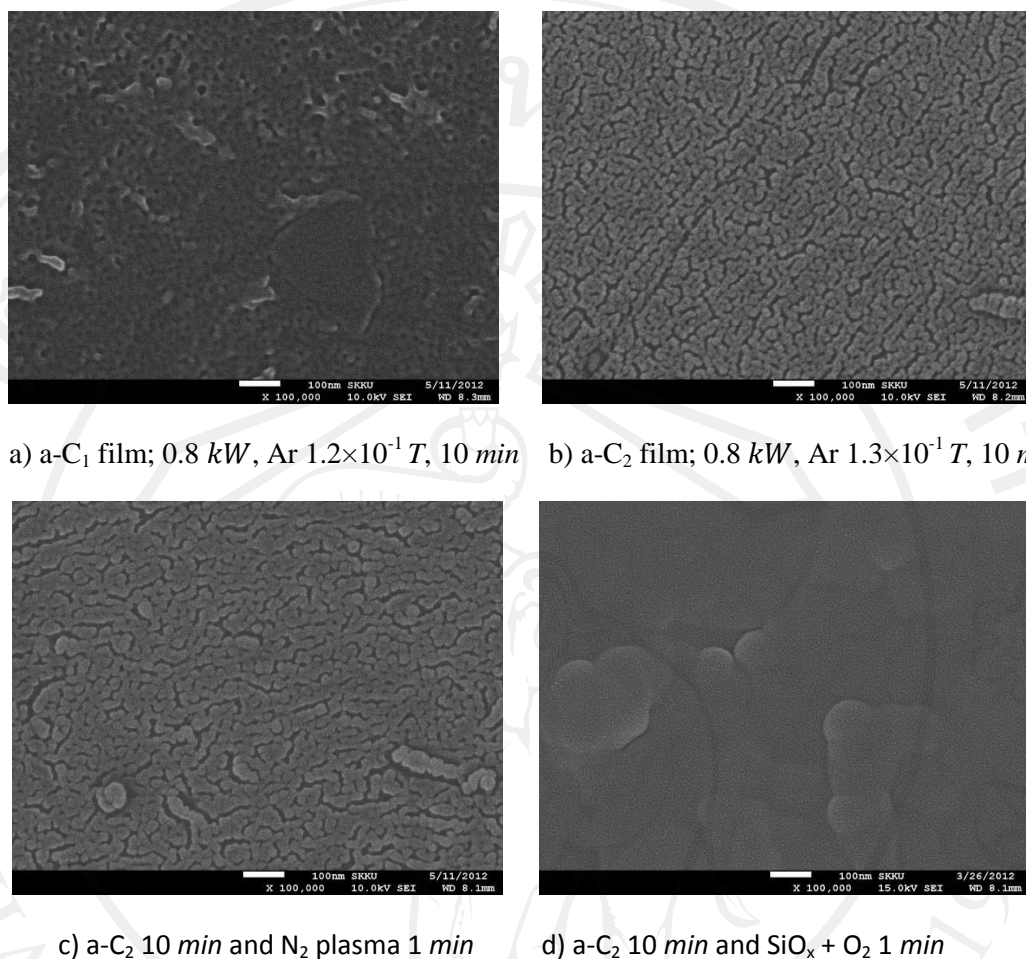


Figure 3.9 SEM images of different types of a-C surfaces.

To study the adsorption of proteins on a rough surface, the physical explanation for the increase in adsorption as surface roughness had to be provided. Basically, a protein has a definite size and shape, more like a colloidal particle, whereas a simple polymer in solution behaves like a random coil. So the studies of simple polymers with high values of surface roughness enhanced adsorption because the polymer can bind several places on a rough surface without losing too much conformation entropy, do not necessarily apply to proteins [17]. Several experimental investigations of protein adsorption on rough substrates exist. All these conclusions were that the height of the nanostructures (the *rms* roughness) should be between 1-2 nm in order to enhance protein adsorption compared to a flat surface. For higher values of 4 nm, adsorption decreases again [18]. This is in agreement with AFM images showed the surface roughness of a-C based-films are about 1.0-1.5 nm, as shown in Figure 3.10.

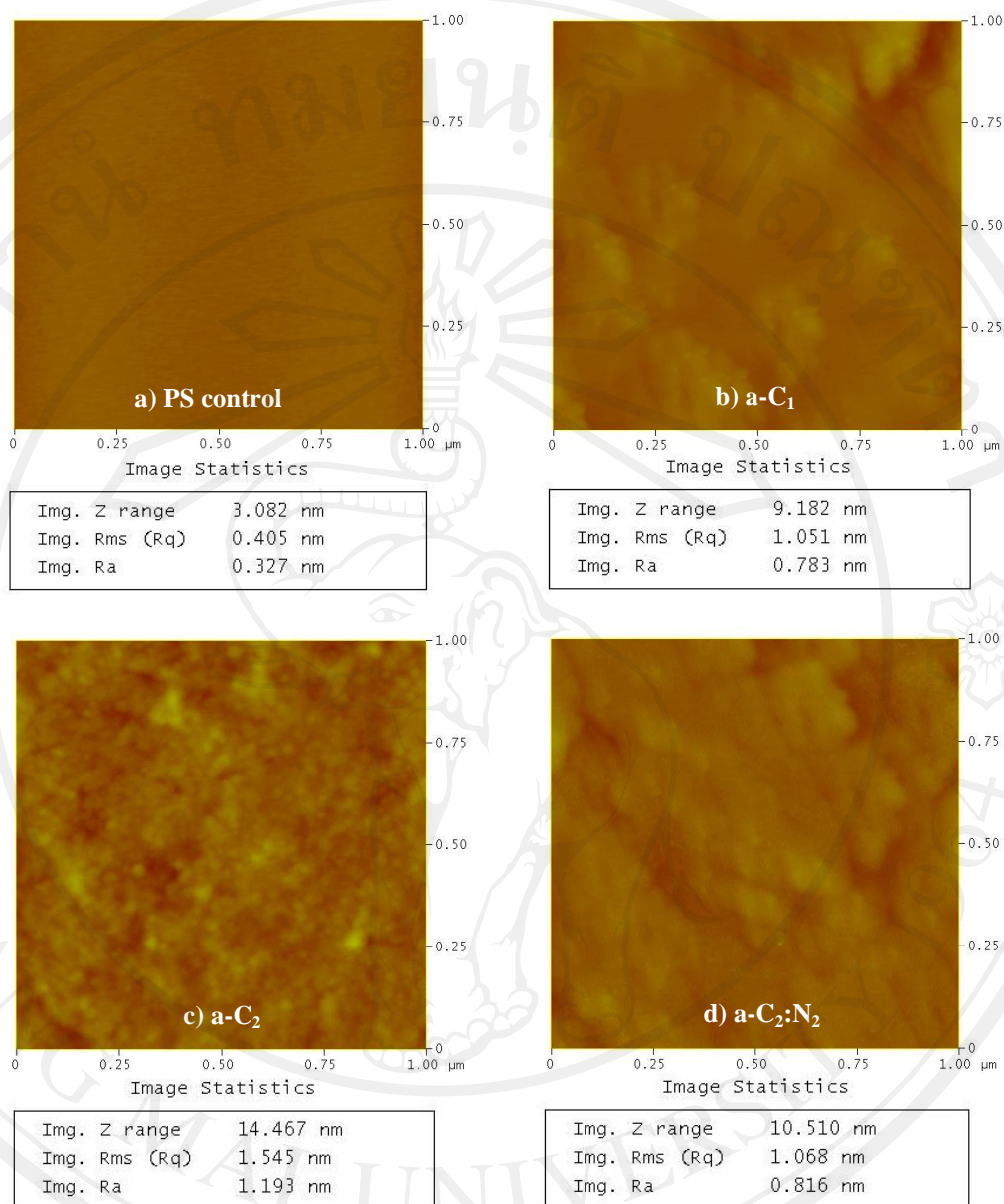


Figure 3.10 AFM images of a-C based-films.

For FTIR analysis, the plasma-modified PS surfaces have been characterized by ATR-FTIR. The absorption spectra of the sericin-coated onto amorphous carbon-based films on PS surfaces are shown in Figure 3.11. The presence of amine functional groups of sericin protein were indicated by the peaks of NH stretching absorption at  $3420\text{--}3440\text{ cm}^{-1}$  region and  $1530\text{--}1560\text{ cm}^{-1}$  region. The peak at  $2080\text{--}2200\text{ cm}^{-1}$  revealed the ketene group of carbon coated-surfaces and the peak at  $1050\text{ cm}^{-1}$  revealed the Si-O bond of  $\text{SiO}_x$  based-films. The aromatic ring of PS structure is indicated by the peak of the absorption at  $1598\text{ cm}^{-1}$  region [17, 18].

The XPS result (Figure 3.12), the survey spectra confirmed the presence of  $C1s$  and  $O1s$  of PS control, demonstrating the oxygen-containing pretreatment onto the PS surface [19] and the presence of  $C1s$ ,  $O1s$  and  $N1s$  of sericin-coated PS surfaces. Table 3.4 shows the surface element composition of PS control and sericin-coated PS surfaces, it can be clearly seen that up to 10% of nitrogen-containing groups from sericin protein were replaced on the amorphous carbon-coated surface after PBS solution washing out the ungrafted molecules. On the XPS analysis, we considered and discussed our results here in the stability of covalent grafting of sericin molecules onto amorphous carbon film and PS surface after washing out. Figure 3.13 shows the high-resolution  $C1s$  spectra of PS control (Figure 3.13a), PS control+sericin (Figure 3.13b), PS+a- $C_1$  (Figure 3.13c), PS+a- $C_1$ +sericin (Figure 3.13d), PS+a- $C_2$  (Figure 3.13e), PS+a- $C_2$ +sericin (Figure 3.13f), PS+a- $C_2:N_2$  (Figure 3.13g) and PS+a- $C_2:N_2$ +sericin (Figure 3.13h). The  $C1s$  peak of PS control (Figure 3.13a) was deconvoluted into six peaks with binding energies of 284.6, 285.2, 285.9, 286.7, 288.5 and 292-293 eV, which were attributed to carbons in  $C-H$  aromatic ( $C=C$ ),  $C-H$  aliphatic ( $C-C$ ),  $C-H_2$ ,  $C-O$  or  $C-OH$ ,  $C=O$  and  $\pi-\pi^*$ , respectively [20, 21]. The  $\pi-\pi^*$   $C1s$  peak is due to “shake-up” excitations taking place in the  $\pi$  orbitals on the benzene rings [21]. Sericin-coated onto PS control surface (Figure 3.13b) produced three new peaks with binding energies of 287.6, 289.2 and 290.3 eV, which were attributed to  $C-NH_2$  (amine) or  $C-O-C$  or  $C-OH$ ,  $C=O$ , and  $O-CO-O$  groups, respectively. Amorphous carbon (a- $C_1$  and a- $C_2$ ) (Figure 3.13c and 3.13e) produced the new peak with binding energy of 286.2 eV, which attributed to  $C-O-C$  group and increased the intensity of  $C=O$  peak at 288 eV especially, a- $C_2$  showed the  $COOH$  peak at 289.3 eV. In the case of a- $C_2:N_2$ , showed the new peak of amide group ( $N-C=O$ ) at 288.5 eV. For sericin-grafted on carbon-coated PS surfaces created three main peaks of  $C-NH_2$ ,  $C-O-C$ ,  $C-OH$ ,  $C=O$ ,  $N-C=O$ ,  $O-CO-O$  groups.

In combination of FTIR and XPS results, it was shown that a-C based films have higher % N atomic mole fraction than PS control, especially, in the case of a- $C_2:N_2$  and a- $C_2$  films. A- $C_2$  and a- $C_2:N_2$  films were porous structures and roughness surfaces which lead to enhancement of the adsorption of sericin proteins. It revealed that functionalized carbon can be enhanced of specific molecules. Moreover, due to the nitrogen-containing groups such as amine group ( $-NH_2$ ) of a- $C_2:N_2$  film, a positively charged, is highly reactive and therefore believed to covalently couple with protein molecules in aqueous environments [8, 17, 22]. Which corresponds with FTIR result, a-C based films produced the peak of ketene groups ( $C=C=O$ ) at wavenumber of 2080-2200  $cm^{-1}$ . Ketene and aminoketene ( $(NH_2)C=C=O$ ) are highly reactive and transient intermediates in a variety of reactions [23].

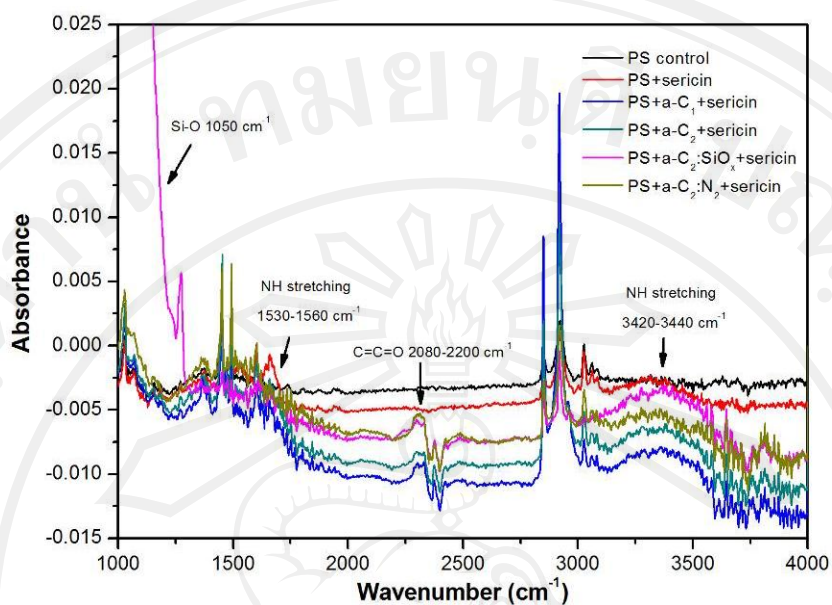


Figure 3.11 Infrared spectra of the PS control and modified-PS coated with sericin surfaces.

Table 3.4 XPS surface elements analysis of PS control and PS coated with sericin after washing out.

	Atomic mole fraction (%)			Atomic ratio
	C	O	N	N/C
PS control	91.69	5.90	-	-
PS control+sericin	72.50	16.04	7.57	0.10
PS+a-C <sub>1</sub> +sericin	67.40	20.10	9.97	0.15
PS+a-C <sub>2</sub> +sericin	67.09	18.62	10.87	0.16
PS+a-C <sub>2</sub> ;N <sub>2</sub> +sericin	59.08	22.43	13.53	0.23

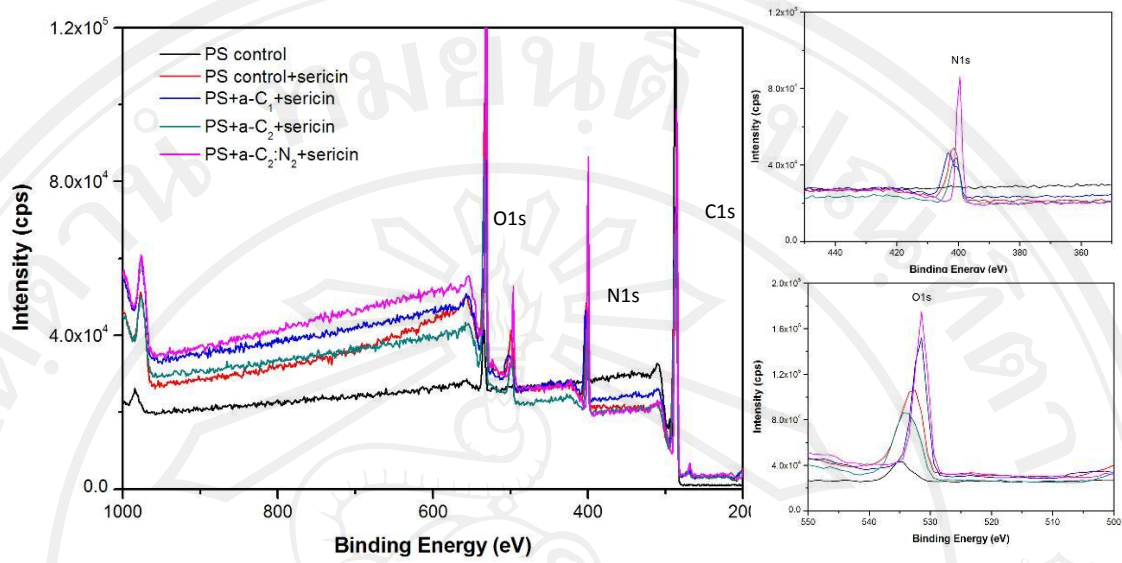
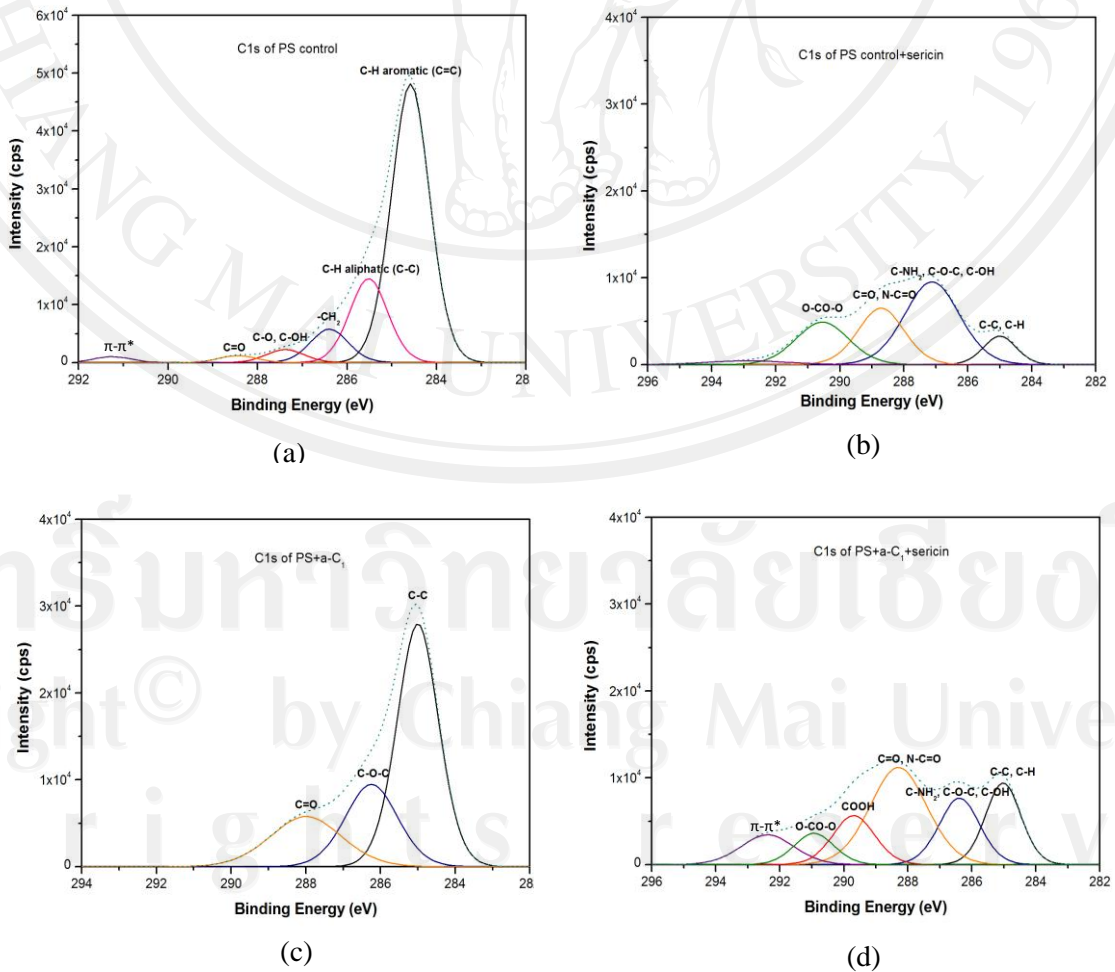


Figure 3.12 XPS scan spectra of PS control and modified-PS coated with sericin surfaces.



(c)

(d)



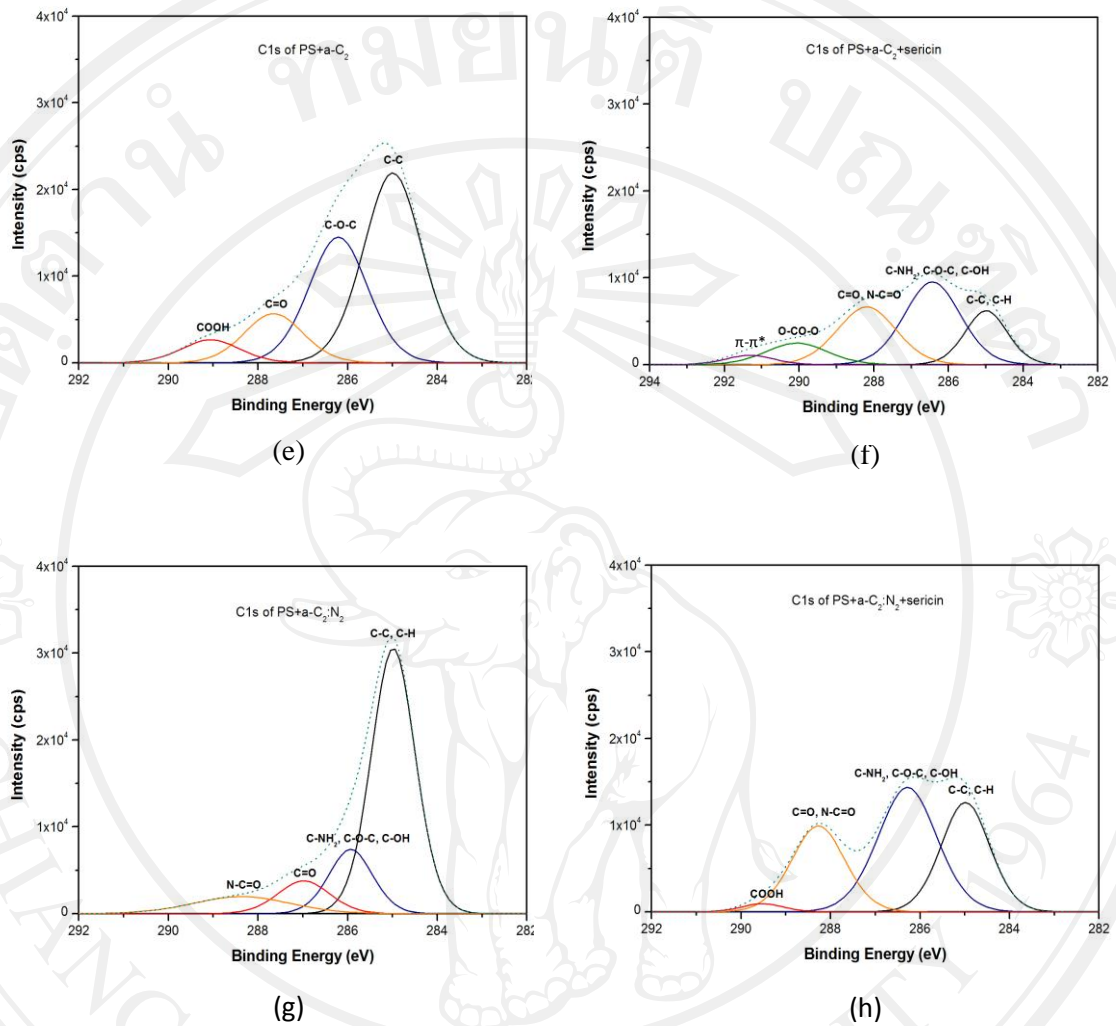
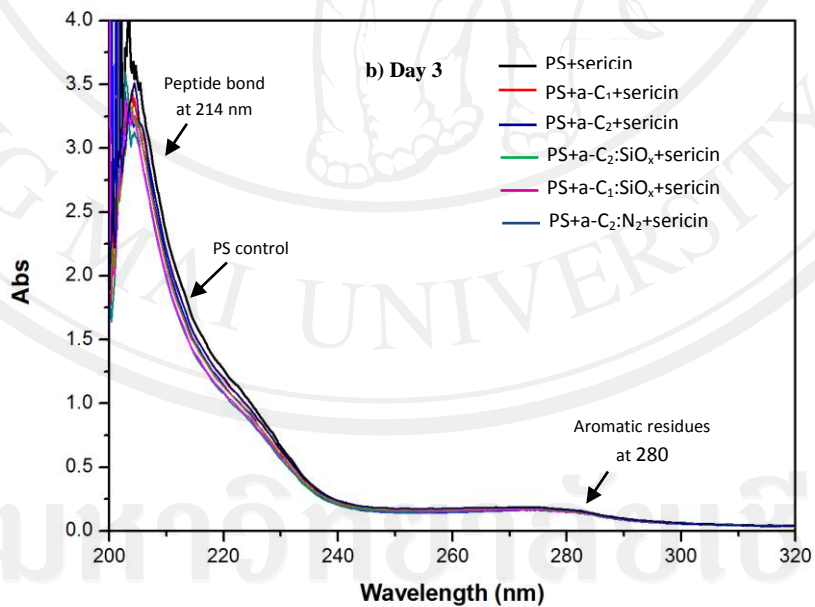
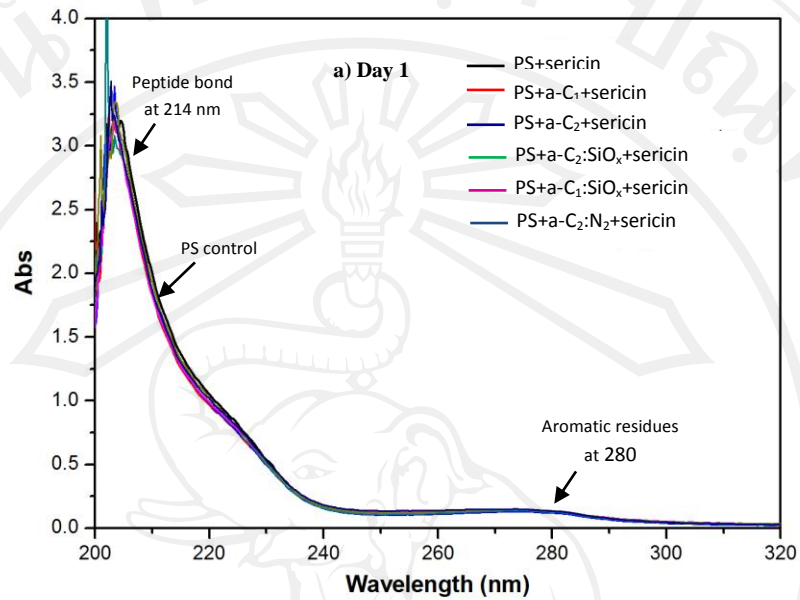


Figure 3.13 High resolution peaks of C1s for PS control and modified-PS coated with sericin surfaces.

### 3.5.2 The Release Rate Detection of Sericin Molecules into PBS Solution.



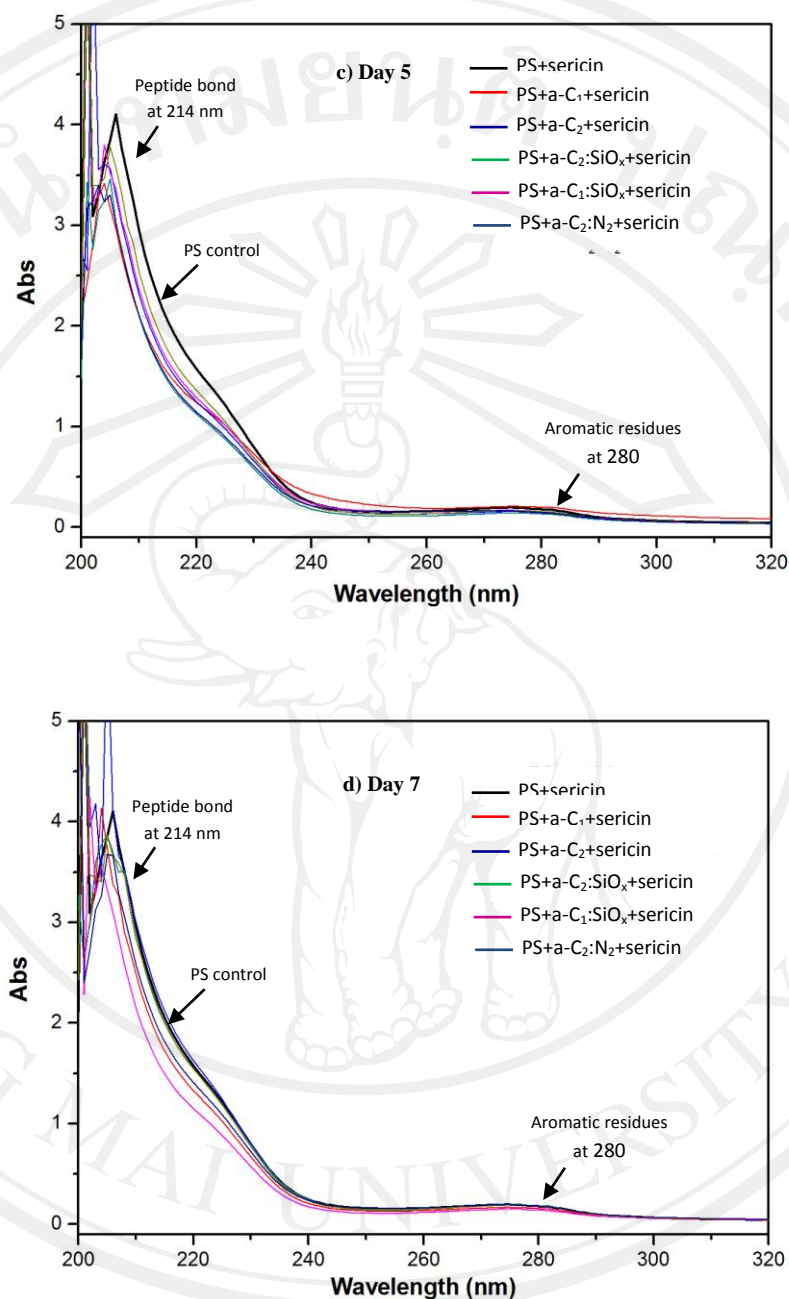


Figure 3.14 UV absorption spectrum of the released-sericin solution.

UV absorbance of the released-sericin solution were scanned with the scanning range was recorded between 190 - 450 nm as shown in Figure 3.14. The amino acids composition of sericin contained a high serine content accounting for about 27.3% of the 18 kinds of amino acids. Serine has strongly polar hydroxyl groups, and is possibly related to the functional and physiochemical properties of sericin [3]. It was

also found the aspartic acid and glycine content accounting for 18.8% and 10.7%, respectively, which indicated that aspartic acid and glycine were also important amino acids attributed to the functions of sericin. In addition, the hydrophilic amino acid amounts up to 70% of the 18 kinds of amino acids, which could account for the good solubility and water absorbability of sericin. It was also found that the amount of aromatic amino acids in sericin was very low (accounting for 6.6% of the 18 kinds of amino acids) compared with other proteins, and this was confirmed by the ultraviolet absorption spectrum. As shown in Figure 3.14, the maximal absorption wavelength was at 214 nm which indicated that peptide bonds were the major absorbing group for sericin in the ultraviolet region, not at 280 nm which assigned to aromatic amino acids absorption wavelength.

For the release rate detection of released-sericin solution, it also found that all of sericin coating onto modified-PS culture dishes have lower released rate of sericin compounds into the PBS solution than PS control for the immersed time at day 1 (Figure 3.14a), day 3 (Figure 3.14b), day 5 (Figure 3.14c) and day 7 (Figure 3.14d). It be implied the covalent bonds interaction between the a-C<sub>1</sub>, a-C<sub>2</sub> as intermediate layer on PS surfaces and sericin coatings can slow down the release rate of sericin compound into the immersed-solution, due to the porous and pore structures and the reactivity functional groups surfaces. It can also reveal that carbon materials appear more attractive for protein adsorption due to their inherent stability and surface properties such as high surface area. Besides the pore structure, the surface functional groups of the carbon are also exceeding parameter that should be taken into account [16].

### 3.5.3 Cell Behavior Study

#### 1) Serum Condition (20% Fetal Bovine Serum; FBS)

Cell behavior experiments were performed over 7 days using hBM-MSCs. Figure 3.15 shows the proliferation pattern of hBM-MSCs with serum condition (20% FBS mixed with 5% sericin) at day 1 and day 7. Day 1 shows the percentage of attached cells on the PS surfaces when cultured for 24 hrs. compared with PS-control. Less adhesion was observed on the three groups of a-C:Si-O<sub>x</sub>-based (silica surface) films as shown in Figure 3.16, and also appeared the rounded-cells which indicated the incomplete attachment of hBM-MSC with ragged cytoplasmic boundary. The silica surface has the strong electrostatic attraction between surface silanol groups and the surface charge of non-prosthetic residues of protein molecules may alter the damage the coherent structure and the native state of the protein [16]. Moreover, silica has the weak stability upon prolonged exposure to aqueous solutions which remains still a major problem in the case of cell culture. It may also conclude that the biological activity and stability of the sericin protein may change upon interaction

with a silica surface. In this case, used hBM-MSCs cultured in a mixture of FBS and sericin coating, it was shown the non significant improvement of proliferation pattern and it can also implied that this culture condition is not supported cell growth rate of hBM-MSCs.

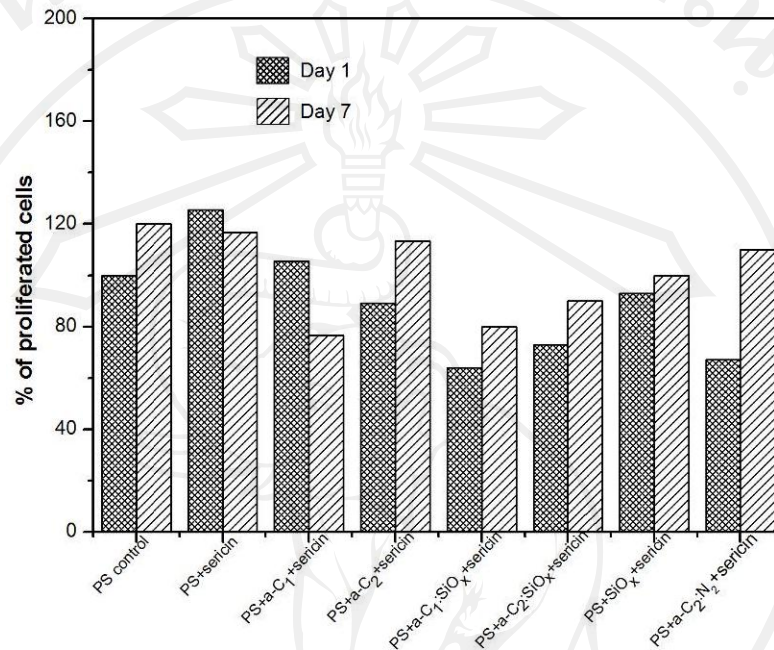


Figure 3.15 Cell proliferation patterns of hBM-MSCs on PS surfaces when cultured in serum condition with 20% FBS and 5% sericin coating at day 1 and day 7.

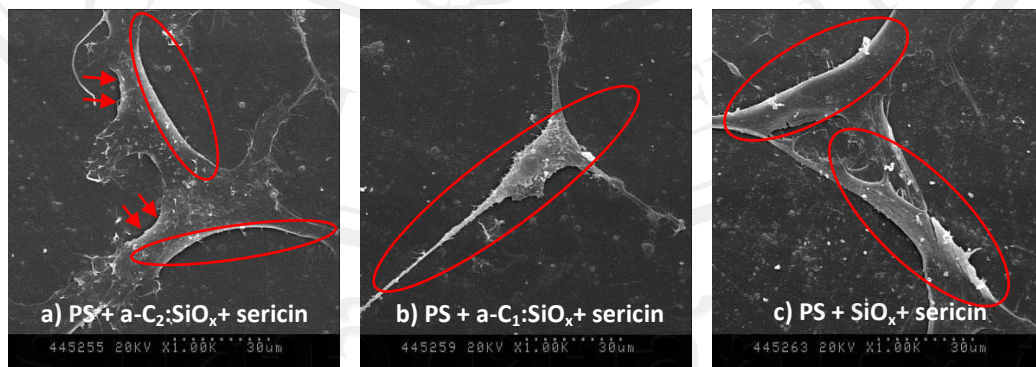


Figure 3.16 Examples of SEM micrographs of attached hBM-MSCs on silica-based surfaces.

## 2) Serum-free Condition (Silk Sericin Protein)

Cell behavior experiments of serum-free condition were performed over 7 days using hBM-MSCs with silk sericin coatings. Figure 3.17 shows the proliferation pattern of hBM-MSCs at day 1 and day 7 with the 5% sericin coatings and mixed with

5% FBS and without FBS conditions. It was shown that PS control dish with 10% FBS has the highest % of proliferated cells at day 7 whereas at day 1, all conditions are not different, it may also reveal that sericin protein and FBS effect on cell attachment in the same way. The carbon-based with sericin-coated surfaces have the higher proliferation rate with the mixed of 5% FBS and sericin coatings and the without FBS than the PS control coated with sericin at day 7 especially, in the case of a-C<sub>2</sub> surface. However, PS dishes with the mixture of 5% FBS and sericin showed the higher proliferated cells than the used of only sericin in the same condition. According with SEM images were shown in Figure 3.18, the attached cell on PS control (Figure 3.18a) showed the ragged boundary (red arrows) were often among cells which indicating the incomplete attachment more than the carbon-based surfaces (Figure 3.18c, 3.18b and 3.18c). It can imply that a-C based films with N<sub>2</sub> plasma treatment (a-C<sub>2</sub>:N<sub>2</sub>) are highly specific binding with sericin molecules, due to its nitrogen-containing groups, however, it can not support the cell growth for a prolonged time. While a-C<sub>2</sub> films show the significantly proliferated cells number at day 7 due to its roughness and porous surfaces.

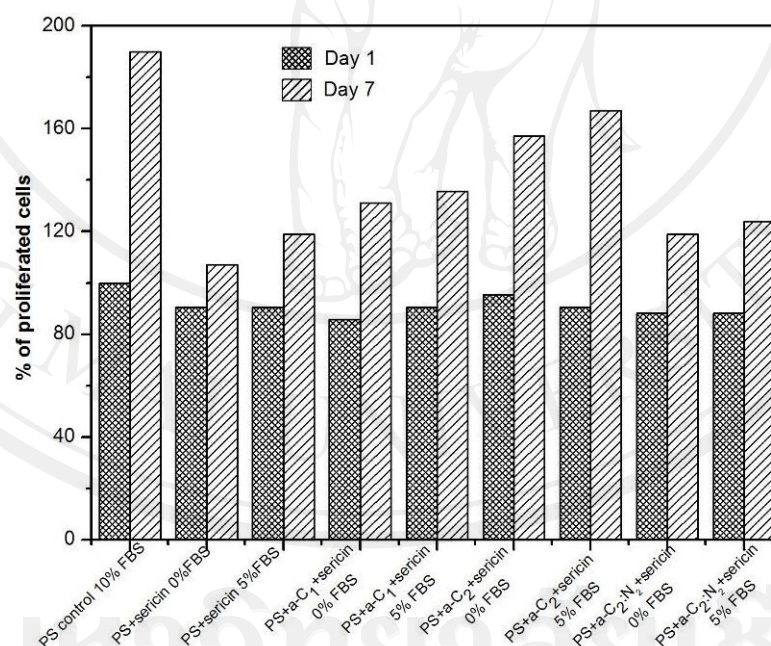


Figure 3.17 Cell proliferation patterns of hBM-MSCs on PS surfaces when cultured in serum-free condition at day 1 and 7.

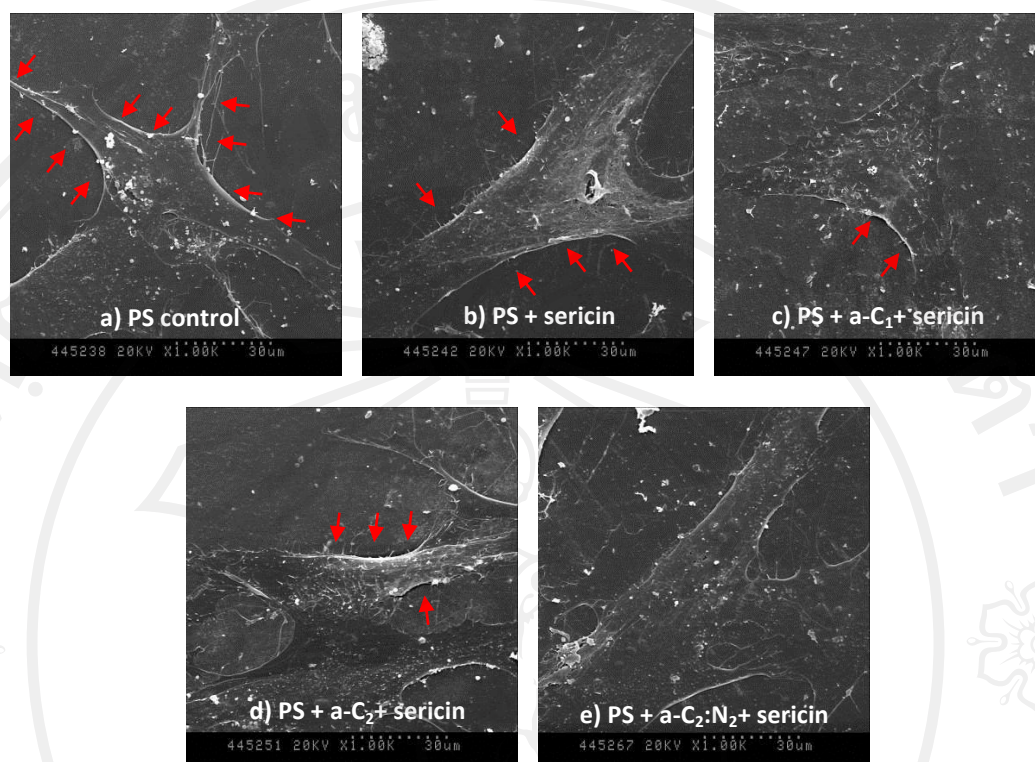


Figure 3.18 Examples of SEM micrographs of attached hBM-MSCs in serum-free condition.

### 3.6 Conclusions

In this study, amorphous carbon based films were used as intermediate layers for covalent grafting between sericin protein and PS surface and also were successfully slow down the release rate of sericin molecules into PBS solution. The Si-O and nitrogen-functional groups great affect to the hydrophilic property of surface more than the roughness of a-C based films. The Si-O groups also influence to surface by made the smooth surface of carbon film and disfavor with hBM-MSCs adherance. The stability of carbon based films with sericin grafting which is more resistant to structural change by hydrolytic effects in aqueous environments and biocompatibility could used in hBM-MSCs culture with serum-free condition. Amorphous carbon material is attractive material for biomolecules adsorption due to its high specific surface area and rough structure in range 1-2 nm and lead to an increase in the total amount of sericin protein absorbed and has the significantly proliferated-cells number at a prolonged time.

**REFERENCES**

- [1] Jennie P.M. *Method in cell biology: Stem cell culture*, 86, ISBN: 978-0-12-373876-9. 2008.
- [2] Wataru S., Ken F., Kana Y., Masahiro S., Yoshihiro K. and Satoshi T. Mitogenic effect of sericin on mammalian cells. *BioMed Central Proceedings*. 2011; 5(Suppl 8): 121.
- [3] Satoshi T., Taeko N., Masahiro S., Hideyuki Y. and Masao M. Sericin, a protein derived from silkworms, accelerates the proliferation of several mammalian cell lines including a hybridoma. *Cytotechnology*. 2002; 40: 3-12.
- [4] Kozo T., Yumiko I., Yoko T. and Hiromi Y. Sericin enhances attachment of cultured human skin fibroblasts. *Biosci. Biotechnol. Biochem*. 2005; 69(2): 403-405.
- [5] Rubin H. Altering bacteriological plastic petri dishes for tissue culture use. *USPHS Rep*. 1966; 81: 843-844.
- [6] Kristian W., Karsten S., Ulrike L. and Andreas O. Plasma-based modification of polystyrene surfaces for serum-free culture of Osteoblast cell lines. *Plasma Process. Polym*. 2006; 3: 524-531.
- [7] Paul D.D. and Jeffrey A.H. *Surface Immobilization of adhesion ligands for investigations of cell-substrate interactions*, The biomedical engineering handbook: Second edition. 2000.
- [8] Ming N., Wen H.T., Deepak C., Nur Nida Abdul R., Ciprian I. and Hanry Y. Cell culture on MEMS platforms: A review. *Int. J. Mol. Sci*. 2009; 10: 5411-5441.
- [9] Hyun-Uk L., Ye-Sul J., Se-Young J., So-Young P., Jong-Seoung B., Hyun-Gyu K. and Chae-Ryoung C.. Role of reactive gas in atmospheric plasma for cell attachment and proliferation on biocompatible poly  $\epsilon$ -caprolactone film. *Appl. Surf. Sci*. 2008; 254: 5700-5705.
- [10] Goddard J.M. and Hotchkiss J.H. Polymer surface modification for the attachment of bioactive compounds. *Prog. Polym. Sci*. 2007; 32: 698-725.
- [11] Hari S.B., Jagannath D., Chowdhury D.P., Reddy A.V.R., Uday C.G., Arvind K.S. and Nihar R.R. Covalent immobilization of protein onto a functionalized hydrogenated diamond-like carbon substrate. *Langmuir*. 2010; 26(22): 17413-17418.
- [12] Su B. J., Yoon S. C., In S. C. and Jeon G. H. Surface energy modification of  $\text{SiO}_x\text{C}_y\text{H}_z$  film using PECVD by controlling the plasma processes for OMCTS ( $\text{Si}_4\text{O}_4\text{C}_8\text{H}_{24}$ ) precursor. *Thin Solid Films*. 2011; 519: 6763-6768.



[13] Parizek M., Kasalkova N., Bacakova L., Slepicka P., Lisa V., Blazkova M. et al. Improved adhesion, growth and maturation of vascular smooth muscle cells on polyethylene grafted with bioactive molecules and carbon particles. *Int. J. Mol. Sci.* 2009; 10(10): 4352-4374.

[14] Kasalkova N., Kolarova K., Bacakova L., Parizek M., Svorcik V. Cell adhesion and proliferation on modified polyethylene. *Mater. Sci. Forum.* 2007; 567-568: 269-272.

[15] Reznickova A., Kolska Z., Hnatowicz V., Stopka P., Svorcik V. Comparison of glow argon plasma-induced surface changes of thermoplastic polymers. *Nucl. Inst. Meth. Phys. Res. B.* 2011; 269(2): 83-88.

[16] Munusami V., Roger C., Karine A., Camelia G., Cathie V-G, Hironori O., Takahi K. and Sumlak I. The influence of surface chemistry and pore size in the adsorption of proteins on nanostructured carbon materials. *Adv. Funct. Mater.* 2010; 20: 2489-2499.

[17] Jin-Hong W., Zhang W. and Shi-Ying X. Preparation and characterization of sericin powder extracted from silk industry wastewater, *Food Chemistry.* 2007; 103: 1255-1262.

[18] Lizhen Y., Juan L., Zhenduo W., Zhongwei L., Qiang C. Calibration of amine density measurement on plasma grafting PET surface and its cell adsorption behaviour. *Surf. Coat. Tech.* 2010; 205: S345-S348.

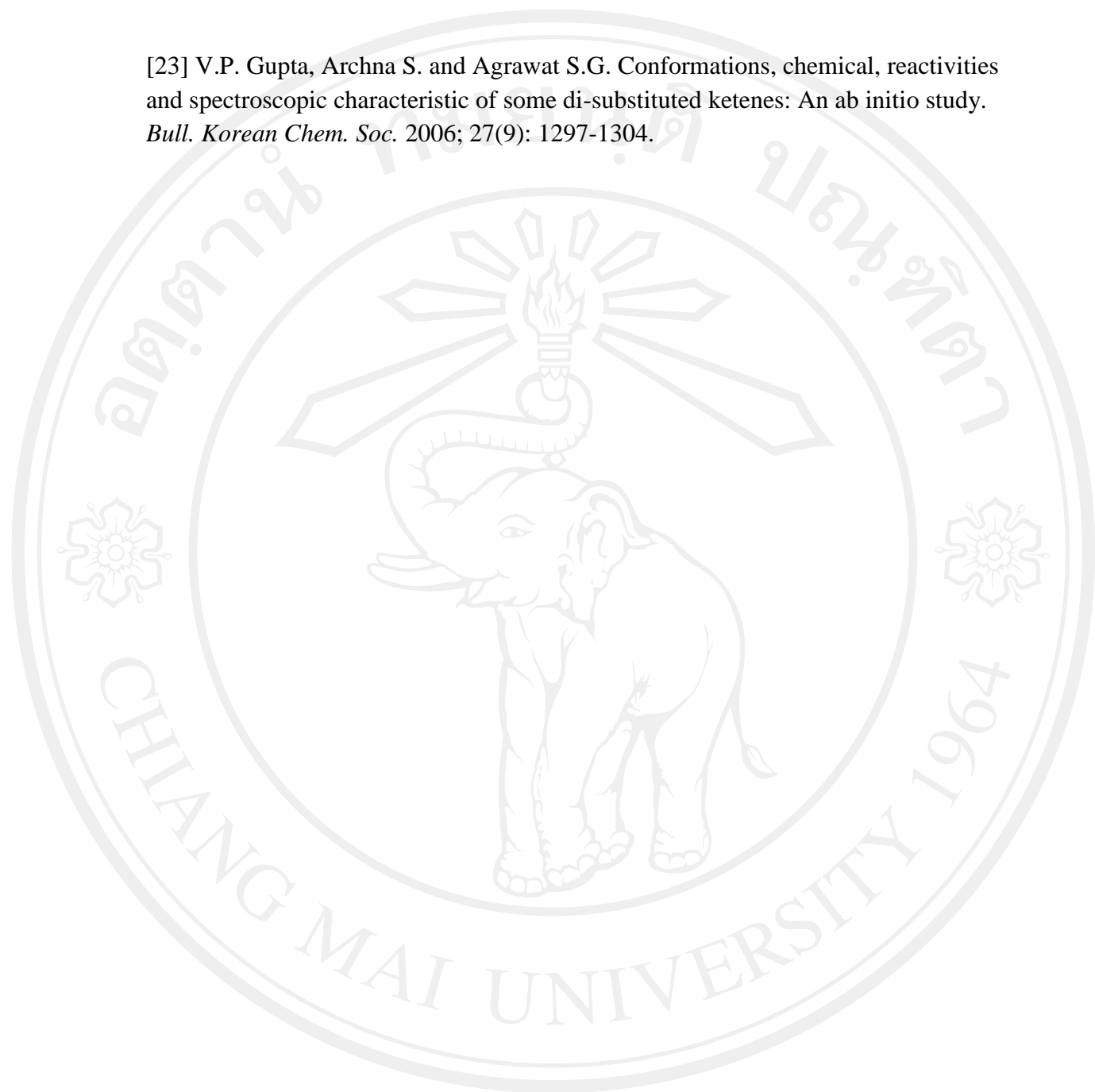
[19] Schamberger P.C., Abes J.I., Gardella Jr J.A. Surface chemical studies of aging and solvent extraction effects on plasma-treated polystyrene. *Colloids Surf. B Biointerfaces.* 1994; 3: 203-15.

[20] Yasushi S., Natsuko M., Shin-ichi K. and Masayuki K. Introduction of carboxyl group onto polystyrene surface using plasma techniques. *Surf. Coat. Technol.* 2008; 202: 5724-5727.

[21] Delphine M., Claude P., Patrick B., Michele S., and Francois R. Synthesis of polystyrene thin films by mean of an atmospheric-pressure plasma torch and a dielectric barrier discharge. *IEEE Transactions on plasma science.* 2009; 37(6): 951-960.

[22] Jinmo K., Donggeun J., Yongsup P., Yongki K., Dae W.M., Tae G.L. Quantitative analysis of surface amine groups on plasma-polymerized ethylenediamine films using UV-visible spectroscopy compared to chemical derivatization with FT-IR spectroscopy, XPS and TOF-SIMS. *Appl. Surf. Sci.* 2007; 253: 4112-4118.

[23] V.P. Gupta, Archana S. and Agrawat S.G. Conformations, chemical, reactivities and spectroscopic characteristic of some di-substituted ketenes: An ab initio study. *Bull. Korean Chem. Soc.* 2006; 27(9): 1297-1304.



ลิขสิทธิ์มหาวิทยาลัยเชียงใหม่

Copyright© by Chiang Mai University  
All rights reserved